Original scientific paper

Redox mediation at poly(*o*-aminophenol) coated electrodes: mechanistic diagnosis from steady state polarization curves

Gabriel Ybarra[1,✉], Carlos Moina[1], María Inés Florit[2], Dionisio Posadas[2]

[1]*Instituto Nacional de Tecnología Industrial, Av. Gral. Paz 5445, CC 157, WAB1650B San Martín, Argentina*
[2]*Instituto de Investigaciones Fisicoquímicas Teóricas y Aplicadas (INIFTA), Facultad de Ciencias Exactas, Universidad Nacional de La Plata, Suc. 4, CC 16, (1900) La Plata, Argentina*

✉Corresponding author - E-mail: gabriel@inti.gov.ar; Tel./Fax: +51-11-4724-6333

Abstract
In this work, the mediated reduction of Fe(CN)$_6^{3-}$ and Fe^{3+} in poly(o-aminophenol) coated electrodes is analyzed by means of a diagnosis diagram based on the features of the steady state current-potential curves. This analysis allows to identify the current determining process and to reproduce the experimental characteristics of the polarization curve from the relevant kinetic and thermodynamic parameters with a minimum amount of experimental measurements.

Introduction

Redox mediation is a process of indirect electron transfer between a redox species in solution and an electrode with the necessary participation of a third actor, a redox mediator [1-5]. Redox mediators can be surface immobilized sites which can be oxidized or reduced electrochemically by controlling the potential of the supporting electrode. The redox sites of the mediator may then oxidize or reduce other redox species in the solution. Direct oxidation or reduction at the electrode surface can be inhibited either because of intrinsically slow heterogeneous electron transfer kinetics or because close approach of the soluble redox species to the electrode is prevented. Redox polymers, such as poly(*o*-aminophenol) (PAP) [2] and Os(II) bipyridyl polyvynilpyridine [6], can act as this kind of surface-immobilized redox mediators.

Redox mediation has attracted the attention of many researchers [4-15], mainly because the possibility of tuning the electrochemical reactivity of the coated electrode towards a specific end,

both by choosing appropriate redox mediators and by controlling the film characteristics. It is also possible to design mediators with certain specific properties, such as ion selectivity, conductivity, formal potential, *etc.*

Several models have been developed to explain the obtained *i-E* curves and the mechanism of mediation. Most of them employ the limiting current obtained in steady state conditions as the only criteria to determine the current determining process. In a previous work [1], we have presented a model, based on the previous work of Laviron [16] and Murray [17], which allows to interpret most of the experimental facts, as well as to elaborate diagnostic criteria from which the kinetic parameters can be estimated. In this work, we show how those diagnostic criteria can be applied to the case of the reduction of $Fe(CN)_6^{3-}$ and Fe^{3+} mediated by a redox polymer. The approach presented here provides a considerable knowledge of the system's electrochemical behavior with a minimum amount of measurements.

Experimental

Analytical grade chemicals were used as received. The solutions were prepared with water purified from a Millipore Milli-Q system. The working electrode was an Au disk with a diameter of 5.0 mm. A PAR Model 273A potentiostat was used for the voltammetric measurements. The counter electrode was a Pt foil of about 5.0 cm². A 1.0 M NaCl normal calomel electrode was used as a reference electrode and the values of the electrode potential were converted to the saturated calomel electrode (SCE) scale. The polymeric films were electropolymerized as indicated elsewhere [2] and all measurements were carried out using 0.1 M $HClO_4$ as supporting electrolyte. Films of different thicknesses were obtained by increasing the electropolymerization time. The charge under the cathodic peak was employed as a measure of the polymer thickness according to a relation obtained by ellipsometry [18].

Theoretical framework

We have presented elsewhere [1] a model based on previous treatments [16,17] to analyze current-potential curves of redox mediation at redox polymers coated electrodes. This model considers that any observed current under steady state conditions follows the process schematically shown in Figure 1.
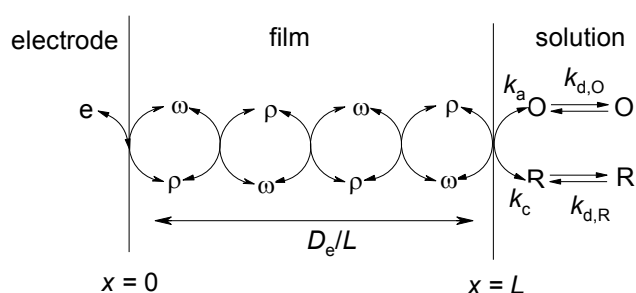
Figure 1. *Schematic representation of the mediation process in redox polymer coated electrodes.*

Oxidized (O) or reduced (R) redox species in solution must reach the polymer-solution interface where an electron transfer reaction takes place with the redox sites in the polymer (ω and ρ stand for the oxidized and reduced species in the polymer). In the solution, species O and R are transported to and from the polymer-solution interface. In steady state conditions, this is usually carried out by controlling the fluxes of O and R with a rotating disk electrode (RDE). After the electron exchange reaction at the polymer-solution interface takes place, charge is transported in

the polymer film by electron hopping, which can be described as a diffusion process. Finally, there is another electron transfer reaction at the polymer-electrode interface, which is assumed to be fast enough as not to be the current determining process. This model is limited to cases were redox species in solution do not penetrate significantly inside the polymer film and can be ascribed to S mechanisms in the Albery's treatment [18].

As has been show before by Laviron [16], there are no thermodynamic restrictions for redox mediation by redox polymers. Nevertheless, coating the electrode with a redox polymer introduces additional processes for the reduction and oxidation of redox agents in solution and, consequently, the *i-E* responses of coated electrodes may differ considerably from those obtained in naked electrodes.

Let us begin considering the electron exchange reaction taking place at the polymer-solution interface:

$$\rho + O \rightleftharpoons \omega + R \tag{1}$$

whose equilibrium constant can be expressed as a function of the formal electrode potentials of both redox couples, $E^{\circ\prime}_{O/R}$ and $E^{\circ\prime}_{\omega/\rho}$, as:

$$K = \frac{\omega C_R}{\rho C_O} = \exp\left(\frac{E^{\circ\prime}_{O/R} - E^{\circ\prime}_{\omega/\rho}}{RT / nF}\right) \tag{2}$$

Unless the value of $E^{\circ\prime}_{O/R}$ is close to that of $E^{\circ\prime}_{\omega/\rho}$, the equilibrium constant will have either a considerably high or a considerable low value and therefore Eq. 1 will be displaced towards the left side (reactants) or the right side (products). We will focus here on mediation processes with high equilibrium constants, as they apply to the cases which will be presented in the Results and Discussion section.

A high equilibrium constant ($K \gg 1$) implies that the reduction of O is greatly favored from a thermodynamic point of view. However, the kinetics of the redox mediation process involves several steps and the actual *i-E* response is determined by all the processes shown in Figure 1. Each of these steps is characterized by parameters which can be expressed as characteristic current values:

$$i_{d,O} = nFAk_{d,O}C_O^S \tag{3}$$

$$i_{d,R} = nFAk_{d,R}C_R^S \tag{4}$$

$$i_e = nFAD_eC_T / L \tag{5}$$

$$i_{kc} = nFAk_cC_TC_O^S \tag{6}$$

$$i_{ka} = nFAk_aC_TC_R^S \tag{7}$$

$i_{d,R}$ and $i_{d,O}$ are related to the transport rate of redox species O and R in solution, i_{ka} and i_{kc} to the charge transfer reaction rate at the polymer-solution interface and i_e to the electronic transport rate in the polymer. C_O^S and C_R^S are the concentration of O and R at the bulk of the solution and $C_T = C_\omega + C_\rho$, the total concentration of redox sites in the mediator (a complete list of symbols is given at the end of the article).

With these five characteristic current parameters, a general relationship for *i-E* curve under steady state can be worked out:

$$i = i_{ka}\left(\theta - \frac{i}{i_e}\right)\left(1 - \frac{i}{i_{d,R}}\right) - i_{kc}\left((1-\theta) + \frac{i}{i_e}\right)\left(1 + \frac{i}{i_{d,O}}\right) \tag{8}$$

where $\theta = C_\omega^0/C_T$ is the fraction of oxidized mediator at the metal-polymer interface.

We may consider that any of the three processes schematically shown in Figure 1 can be the one determining the limiting current. We will denominate case **R** to the conditions in which the electron transfer at the polymer-solution interface is the current determining process (c.d.p.), case **E** to the one which is controlled by slow charge transport in the film, and case **D** to the one which is determined by slow mass transport in the solution.

In all cases, the resulting *i-E* curve obtained from Eq. 8 has the usual sigmoidal shape. However, its location in the potential scale may vary between $E^{0'}{}_{O/R}$ and $E^{0'}{}_{\omega/\rho}$, and the limiting current may vary from null to a certain value which is related to the most sluggish process(es) from those shown in Figure 1. It is interesting to note that the identification of the c.d.p. can be achieved with a minimum of experimental measurements (as few as two) by observing the influence of the film thickness on the value of the half-wave potential $E_\frac{1}{2}$ and the limiting current. Figure 2 shows the diagnostic flow chart which has been worked out to identify the c.d.p.
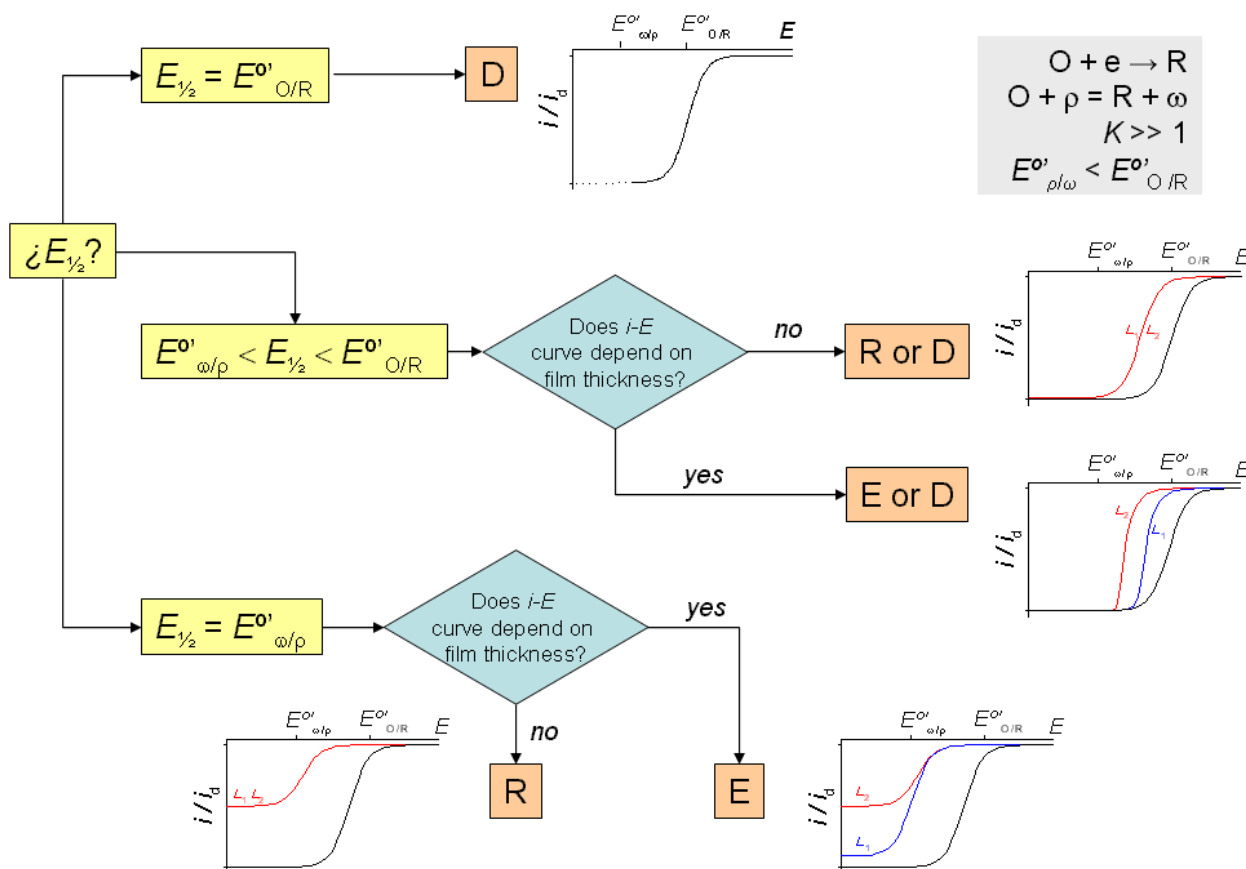
Figure 2. *Diagnostic flow chart based on the consideration of half-wave potential and the film thickness for the mediation of the reduction of an oxidized agent under the conditions stated in the upper right square.*

It is also possible to construct a kinetic diagram, such as the one shown in Figure 3, similar to others previously reported [16]. This kind of diagrams is useful to visualize how experimental variables, such as the concentration of the external redox couple, film thickness and rotation frequency, affect the overall process of mediation. These plots are constructed using characteristic parameters of the system. We have chosen to plot log (i_{kc}/i_e) as a function of log ($i_{kc}/i_{d,O}$) as shown

in Figure 3. For instance, the effect of increasing the film thickness is to slow down the charge transport in the film and correspond to a vertical displacement in the kinetic diagram. Therefore, **R→E** or **D→E** transitions could be observed by increasing the film thickness. Likewise, increasing the rotation frequency of the rotating disk electrode is associated to a horizontal displacement, and **D→R** or **D→E** transitions are to be expected. The use of the diagrams such as those presented in Figure 2 and 3 provide a straightforward insight into the mediation processes of different systems as is shown in the next section.
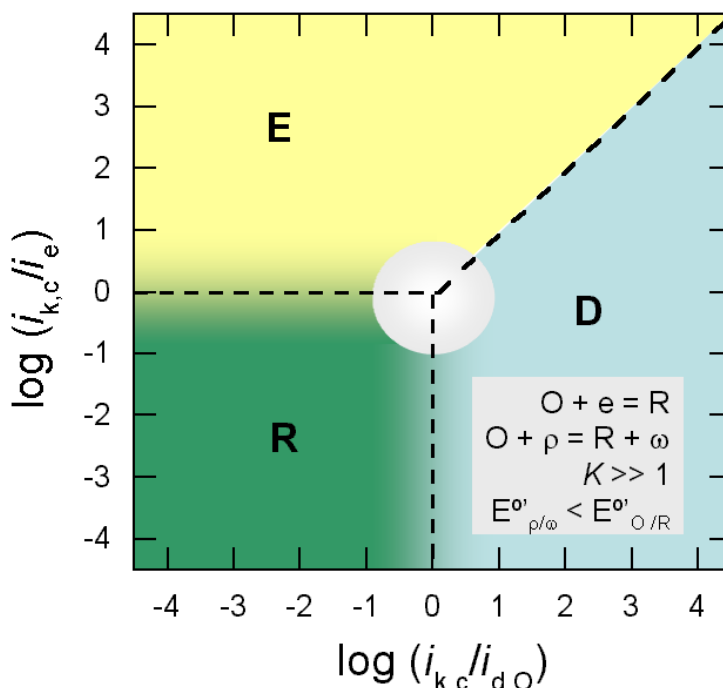

Figure 3. Kinetic scheme showing the three different regions of control of the limiting current.

Results and discussion

We will begin considering the PAP|Fe(CN)$_6^{3-/4-}$ system. Figure 4a shows the steady state current-potential curves obtained for the redox couple Fe(CN)$_6^{3-/4-}$ in 0.1 M HClO$_4$ for a naked and a PAP-coated electrode with different thickness at a constant rotation frequency. Both cathodic and anodic currents can be observed in the naked electrode, and the limiting current value corresponds to that obtained for the diffusion of species in solution. On the contrary, only the cathodic wave, which corresponds to the reduction of Fe(CN)$_6^{3-}$, can be observed in PAP coated electrodes and it is displaced towards more negative potentials when compared to the naked electrode. Besides, it can be seen that the limiting current depends on the film thickness.

We will interpret the obtained results within the frame of the diagnostic flow chart based on the half-wave potential value. The formal potential of the quasi-reversible couple in the redox polymer PAP has been estimated to be +0.050 V *vs.* SCE [2]. It can be seen in Figure 4a that PAP-coated electrodes present only the cathodic wave and that the half-wave potential is displaced towards more negative values as compared with the curve obtained in naked electrodes. In fact, the $E_{\frac{1}{2}}$ obtained with the coated electrode coincides with the value of the formal potential of PAP. It can also be seen that the limiting current depends on the film thickness; the thicker the film, the lower the limiting current. Based on these features of *i-E* curve and following the diagnosis diagram (Figure 2), we reach the conclusion that the electron transport within the film is the current determining step (case **E**).
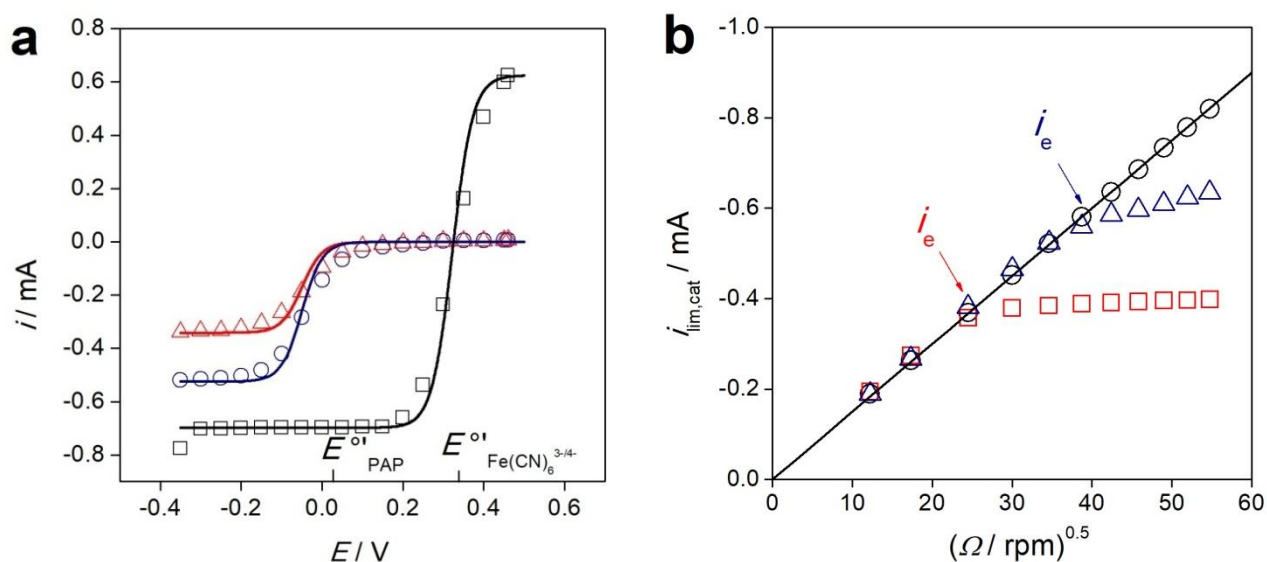
Figure 4. (a) *Experimental steady state i-E curves obtained in a 5 mM Fe(CN)$_6^{3-}$ + 5 mM Fe(CN)$_6^{4-}$ + + 0.1 M HClO$_4$ solution for a Au pristine electrode (□) and coated with PAP with a thickness of 88 nm (○) and 125 nm (△), at a rotation frequency of 1200 rpm. Full lines show simulated i-E curves.* **(b)** *Levich plot for a pristine (——) and PAP coated Au electrode with different film thickness: 163 nm (□), 88 nm (▽), 51 nm (○), obtained in a 5 mM Fe(CN)$_6^{3-}$ + 5 mM Fe(CN)$_6^{4-}$ + 0.1 M HClO$_4$ solution.*

A Levich plot obtained for films with three different thicknesses is shown in Figure 4b. As can be seen, the limiting current increases linearly at low rotation frequency and reaches a constant value for a given thickness. This behavior can be explained by considering that the c.d.p. is the diffusion of Fe(CN)$_6^{3-}$ in the solution at low rotation frequency and then the c.d.p. is the electronic transport in the polymer film at high rotation frequency. The transition between both regimes is abrupt. As long as Fe(CN)$_6^{3-}$ flux does not exceed the electron transport capacity in the film, the limiting current will equal the limiting current observed in naked electrodes; once it is exceeded, the limiting current equals the electron transport current, i_e from Eq. 5.

It is possible to simulate *i-E* curves by employing Eq. 8 and the values of characteristic currents (i_e, $i_{d,O}$ and $i_{d,R}$) as experimental parameters. Being the kinetics of electron transfer much faster than diffusion process, kinetic parameters can be neglected from Eq. 8 ($i_k \gg i_e$, $i_k \gg i_d$); electron transport characteristic current values can be obtained from Figure 4b (i_e = 0.341 mA and i_e = 0.524 mA for the thickest and the thinnest films, respectively); finally, diffusion characteristic current can be obtained from measurements carried out on naked electrodes ($i_{d,O}$ = 0.698 mA and $i_{d,R}$ = 0.625 mA). These parameters, together with the value of the formal potentials for PAP and Fe(CN)$_6^{3-/4-}$ couples, are enough to simulate the *i-E* curve. The simulated curves are shown in Figure 4a.

Let us now consider the PAP|Fe$^{3+/2+}$ system, with 5 mM Fe$^{3+/2+}$ as the external redox couple in a 0.1 M HClO$_4$ solution. The redox couple has a formal potential of $E^{o'}$(Fe$^{3+/2+}$) = +0.510 V *vs.* SCE. The *i-E* curves are shown in Figure 5a, both for naked and PAP-coated electrodes. The *i-E* response for PAP-coated electrodes shows no anodic currents and the cathodic limiting current is independent of the film thickness.

Figure 5a shows the steady state *i-E* curves for the reduction of Fe^{3+} in 0.1 M HClO$_4$ obtained for an Au electrode and a PAP coated electrode at the same rotation frequency. At first sight, the features of these curves are quite similar to those found for the reduction of Fe(CN)$_6^{3-}$, with a displacement of the cathodic wave towards more negative potential. We will employ the diagnosis criteria based on the half-wave potential to sort out the mechanism.
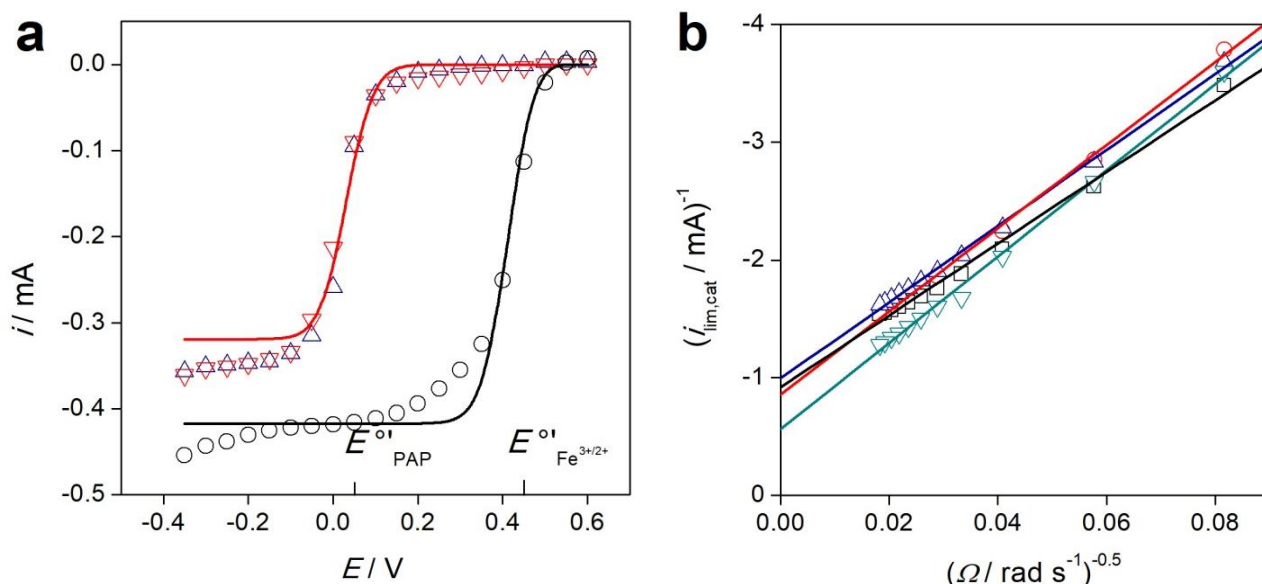
Figure 5.(a) *Experimental steady state i-E curves obtained in a 10 mM Fe(III) + 0.1 M HClO₄ solution for a Au pristine electrode (○) and coated with PAP of 116 nm (up triangle) y 249 nm (down triangle), at a rotation frequency of 300 rpm. Full lines show simulated i-E curves.*
(b) *Koutecky-Levich plot for PAP coated electrodes in a 10 mM Fe(III) + 0.1 M HClO₄ solution. Film thickness: 43 nm (□), 116 nm (△), 249 nm (▽) and 117 nm (○)*

Firstly, it can be noted that the half-wave potential has the same value of the PAP redox couple. Secondly, the limiting current is insensitive to the film thickness. Keeping this in mind, we may now follow the diagnosis diagram and reach to the conclusion that *i-E* curve is a typical Case **R** where the c.d.p. is the electron transfer reaction between the polymer and the redox species.

The Koutecky-Levich plots, $i_{lim,cat}^{-1}$ *vs.* $\Omega^{1/2}$ (Figure 5b), provide additional information for systems which can be ascribed to Case **R**. It can be shown from Eq. 8 that, under circumstances that apply in this case, the origin ordinate equals i_{kc}^{-1}. As was done with the PAP|Fe(CN)$_6^{3-/4-}$ system, the *i-E* curve can be simulated employing as experimental parameters the value of the characteristic current for the electron transfer kinetics (i_{kc}^{-1}) and the diffusion one ($i_{d,R}$), and the formal potential for the PAP couple and the Fe$^{2+/3+}$ redox couple (see Figure 5a).

Finally, it worth noting that it is possible to locate both studied systems PAP|Fe$^{3+/2+}$ and PAP|Fe(CN)$_6^{3-/4-}$ in a kinetic diagram, employing estimated values for the kinetic constants and diffusion coefficients [2]. The axis in the kinetic diagram corresponds to non-dimensional parameters formed by constants (electron transfers constant, diffusion coefficient) and variables (frequency of rotation of the RDE, film thickness). While the involved constants depend exclusively on the system under study, variables can be modified within a certain range. Thus, there is a window accessible for any given system. In Figure 6 we show the estimated windows for both systems. In the case of the PAP|Fe$^{3+/2+}$ system, electron transfer at the polymer-solution interface is so sluggish that this process will always have a determining influence on the observed current (case **R**). On the contrary, for the PAP|Fe(CN)$_6^{3-/4-}$, the electron transfer is so rapid that other processes will limit the current: either the transport of redox agents in solution (case **D**) or the electron transport in the polymer film (case **E**). As a matter of fact, it is possible to move from one regime to the other by controlling the experimental variables. We may change from case **D** to case **E** either by increasing the rotation frequency (*i.e.* moving horizontally in the kinetic diagram) or by increasing the film thickness (moving vertically in the kinetic diagram). In both cases, the transition is abrupt, as shown in Figure 4b.
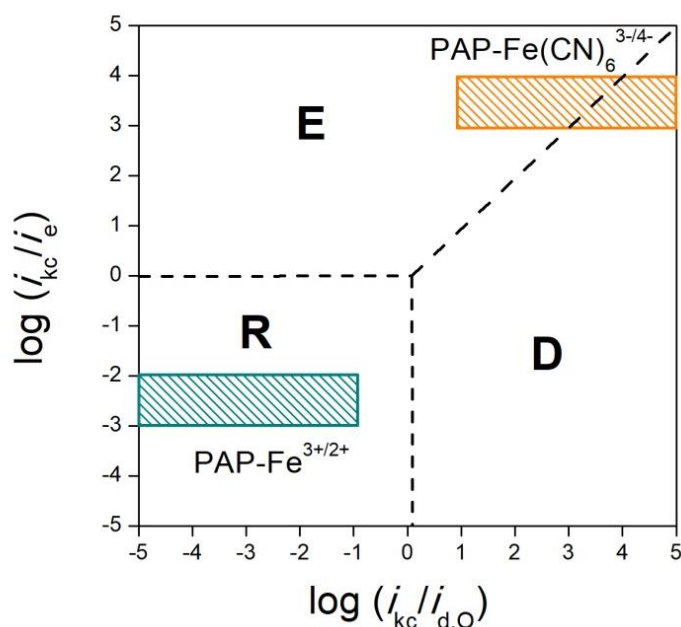
Figure 6. *Localization in the kinetic diagram for the reduction of Fe(III) species in the two PAP-Fe(II/III) systems presented in this work.*

Conclusions

In this work we have analyzed the *i-E* response of a redox polymer (PAP) modified electrode in steady state towards the mediated reduction of Fe^{3+} and $Fe(CN)_6^{3-}$. The available set of diagnostic criteria is widened with the addition of the position of the half-wave potential. We have shown that the analysis of the complete curve allows identification of current determining process, to obtain the kinetic and transport parameters and to simulate the experimentally obtained current-potential curves with a set of characteristic current values which can be easily assessed.

List of symbols

θ	fraction of oxidized redox sites
ρ	reduced redox site in the polymer
ω	oxidized redox site in the polymer
Ω	electrode rotation frequency
A	electrode area
C	concentration
D	diffusion coefficient
E	electrode potential
$E^{o\prime}$	formal potential
$E_{1/2}$	half-wave potential
F	Faraday constant
i_e	characteristic electronic current
i_d	characteristic diffusion current

i_k	characteristic kinetic current
i_{lim}	limiting current
K	electron transfer rate constant
K	equilibrium constant
L	film thickness
N	number of exchanged electrons
O	oxidized species in solution
R	reduced species in solution
R	gas constant
T	absolute temperature
x	distance from the electrode-polymer interface

Subscripts and superscripts

0	metal-polymer interface
A	anodic
C	cathodic
Eq	thermodynamical equilibrium condition
D	diffusion
E	electronic
L	polymer-solution interface
O	soluble oxidized species
R	soluble reduced species
S	solution
T	total redox sites

Current determining processes

Case **E**	control by slow electron transport in the polymer
Case **D**	control by slow soluble species diffusion in the solution
Case **R**	control by slow electron transfer reaction between soluble species and redox species in the polymer

References

[1] G. O. Ybarra, C. Moina, M. I. Florit, D. Posadas, *Journal of Electroanalytical Chemistry* **609** (2007) 129-139.

[2] G. Ybarra, C. Moina, M. I. Florit, D. Posadas, *Electrochimica Acta* **53** (2008) 3955-3959.

[3] G. Ybarra, C. Moina, M. I. Florit, D. Posadas, *Electrochimica Acta* **53** (2008) 4727-4731.

[4] C.P. Andrieux, J.-M. Savéant. *Molecular Design of Electrode Surfaces*, pp. 207-273, Ed. R.W. Murray, Wiley, New York, 1992.

[5] M. E. G. Lyons. *Molecular Design of Electrode Surfaces*, pp. 277-371, Ed. R.W. Murray, Wiley, New York, 1992.

[6] G. Ybarra, C. Moina, E. M. Andrade, F. V. Molina, M. I. Florit, D. Posadas, *Electrochimica Acta* **50** (2005) 1505-1513.

[7] L. Yang, X. Huang, A. Gogoll, M. Strømme, M. Sjödin, *Electrochimica Acta* **204** (2016) 270-275.

[8] S.-W. Lee, J. Lopez, R.F. Saraf, *Electroanalysis* **25** (2013) 1557–1566.

[9] R. Francke, R. D. Little. *Chemical Society Reviews* **43** (2014) 2492-2521.

[10] H. Tokue, K. Oyaizu, T. Sukegawa, H. Nishide. *ACS Applied Materials and Interfaces* **6** (2014) 4043-4049.

[11] K. Oyaizu, H. Tatsuhira, H. Nishide, *Polymer Journal* **47** (2015) 212–219.

[12]   H. Tokue, K. Kakitani, H. Nishide, K. Oyaizu, *RSC Advances* **6** (2016) 99195-99201.

[13]   R. D. Milton, T. Wang, K.L. Knoche, S.D. Minteer, *Langmuir* 32 (2016) 2291-2301.

[14]   H. M. Bambhania, D. Chakraborty, H. Wen, S. Calabrese Barton, *Journal of the Electrochemical Society* **164** (2017) H232-H240.

[15]   H. Tokue, K. Kakitani, H. Nishide, K. Oyaizu, *Chemistry Letters* **46** (2017) 647-650.

[16]   E. Laviron, *Journal of Electroanalyticla Chemistry* **112** (1980) 1- 9.

[17]   T. Ikeda, C. R. Leidner, R.W. Murray, *Journal of Electroanalytical Chemistry* **138** (1982) 343.

[18]   C. Barbero, L. Sereno, J. O. Zerbino, D. Posadas, *Electrochimica Acta* **32** (1987) 693.

[19]   W. J. Albery, A.R. Hillman, *Journal of Electroanalytical Chemistry* **170** (1984) 27.